Dynamics of Continuous Isobutylene Cationic Polymerizations

MARCELO FONSECA DE FREITAS and JOSÉ CARLOS PINTO*

Programa de Engenharia Química/COPPE, Universidade Federal do Rio de Janeiro, Cidade Universitária, P.O. Box 68502, Rio de Janeiro, 21945-970 RJ, Brazil

SYNOPSIS

Polyisobutylene can be produced in either continuous cationic precipitation or solution polymerization reactors. It is known that the open-loop behavior of polymerization reactors may be very complex and may lead to oscillatory behavior, which is usually caused by thermal positive feedback (due to the large heats of reaction of polymerization reactions) and high viscosity effects (such as the gel effect in radical polymerization reactors and the decrease of heat transfer coefficients at high polymer concentrations). Oscillatory behavior may be observed in industrial isobutylene reactors, and it is intended to know whether these oscillations are inherent to the kinetic mechanism. Based on published experimental data, mathematical models are developed for both solution and precipitation processes. Steady-state solutions are calculated and steady-state stability is analyzed. Dynamic simulations and stability results reveal that only single stable steady-state solutions are possible for such reactors at usual operation conditions, which means that oscillatory behavior is not intrinsic to the reaction mechanism. © 1996 John Wiley & Sons, Inc.

INTRODUCTION

The most important commercial cationic polymerization processes are related to the production of isobutylene-based polymers. These polymers include butyl rubbers, polybutenes, and polyisobutylene (isobutylene homopolymer). These processes are usually performed in continuous solution or precipitation reactors, where a Bronsted Acid like $AlCl_3$ or BF_3 is used as a catalyst in an organic solvent at temperatures that range between ambient and very low temperatures (as low as $-100°C$). The polymerization reaction is extremely fast and sensitive to the presence of impurities, especially water, which is assumed to play the role of cocatalyst in the polymerization mechanism.[1,2]

Polyisobutylene is produced commercially by the homopolymerization of isobutylene in continuous precipitation reactors, using $AlCl_3$ as a catalyst and methyl chloride as a solvent. In this case, the reactor is refrigerated by boiling ethylene at $-100°C$ in external heat exchangers (EXXON Process). A second commercial process uses BF_3 as a catalyst in a closed loop moving belt (BASF process—flash polymerization). Solution processes are also used to produce polyisobutylenes, and some of them are described in the literature.[1,2] N-Alkanes are usually used as solvents, and condensers are used to remove the heat released by reaction (autorefrigerated reactors). The catalysts are the same described before.

The operation of isobutylene polymerization reactors is not simple. Kresge reports that some industrial plants are composed of multiple reactors, which are operated intermittently for a maximum of 60 consecutive hours, due to operational problems. Oscillatory behavior and reaction extinction have also been reported by industrial engineers.[3] These problems may be caused by dynamic instabilities, such as those that lead free radical solution polymerization reactors to steady-state multiplicity and oscillatory operation.[4-6] In free radical solution reactions, instabilities are largely caused by a thermal positive feedback, which is due to the large heats of reaction of polymerization reactions. For instance, a small increase (decrease) of reactor temperature

* To whom correspondence should be addressed.

Journal of Applied Polymer Science, Vol. 60, 1109–1126 (1996)
 CCC 0021-8995/96/081109-18

causes an increase (decrease) of reaction rates and, consequently, an increase (decrease) of the amount of heat released by reaction, which leads to an additional increase (decrease) of reactor temperature. This autoacceleration may go out of control, leading the reactor operation to a different steady-state solution or to oscillatory operation. Similar effects may be caused by the increasing (decreasing) viscosities of the reaction medium when monomer conversion increases (decreases). In this case, the heat transfer coefficient may decrease (increase) due to the increasing (decreasing) viscosities, causing an increase (decrease) of the reactor temperature and, simultaneously, of monomer conversion.[7,8] Dynamic instabilities are experimentally observed and theoretically predicted in most polimerization systems, like free radical emulsion,[9] free radical suspension,[10] and gas–phase[11] and slurry[12] Ziegler–Natta reactors.

Isobutylene polymerization reactors have been very poorly studied. It seems that the only work published that regards such reactors is the one by Maschio et al.,[13] which analyzes the solution polymerization in batch isothermal reactors. In this work the authors wrote mass balances and MWD moment equations for dead and growing polymer chains in order to describe monomer conversion and polymer molecular weight distribution.

Thus, the analysis of continuous polyisobutylene reactor model and stability is still lacking. In this work two mathematical models for the continuous isobutylene cationic polymerization reactors are developed: one for the solution (homogeneous) polymerization and another for the precipitation (heterogeneous) polymerization. The models are used to analyze whether complex dynamic behavior is inherent to the kinetic mechanism of cationic isobutylene polymerization or whether it is caused by external variables, such as heat exchanger design and the presence of impurities. Process conditions analyzed are similar to the conditions of the Exxon process for the high molecular weight isobutylene homopolymerization. So, the catalyst is $AlCl_3$, the solvent is methyl chloride for the precipitation reactor and *n*-pentane for the solution reactor, and the operation conditions and reactor geometry are similar to the Exxon industrial systems.

KINETIC MECHANISM

Based on the work of Kennedy and co-workers,[2,14–23] who in the early sixties studied the isobutylene cationic polymerization in detail at conditions that were similar to EXXON industrial polymerizations, Freitas[24] proposed the kinetic mechanism shown in Table I for the isobutylene polymerization.

Nowadays, it is not possible to characterize the identity and concentration of the actual catalyst and cocatalyst in the reaction medium. The initiation step is not completely understood yet, so that the actual catalyst concentration is represented here as a fraction of the total amount of the $AlCl_3$ fed, by means of a catalyst efficiency. According to Plesch,[25] $AlCl_3$ is easily complexed by the monomer when they are mixed, which inhibits the initiation step. Therefore, it is reasonable to assume that the actual catalyst is produced outside the reactor, before the mixing of the monomer and catalyst streams. The propagation step is composed of two parts: the activation (dissociation) equilibrium and the chain growth.[17,19,21,23] The activation equilibrium is due to the ionic nature of the growing species. It is generally accepted that the ions have to be far enough for a monomer molecule to be incorporated into the growing chain. Chain transfer occurs to both monomer and solvent molecules and controls molecular weight.[14,21] According to Kennedy and Squires,[21] only espontaneous unimolecular termination occurs. Although this step has been neglected in previous studies, it is responsible for incomplete monomer conversion and is extremely important to the description of actual process operation. This mechanism may be used to describe homogeneous and heterogeneous polymerizations.

The homogeneous isobutylene polymerization in *n*-pentane was studied by Kennedy and Thomas[15] and Kirshenbaum, Kennedy, and Thomas.[23] The heterogeneous isobutylene polymerization in methyl chloride was studied by Kennedy and co-workers.[2,14,16–21] Due to the molecular polarity of methyl

Table I Isobutylene Polymerization Kinetic Mechanism

Initiation	
Initiator formation	$A + X \overset{K}{\leftrightarrow} A^*$
Chain formation	$A^* + M \overset{k_i}{\rightarrow} P_1$
Propagation	
Activation-deactivation	$P_i \underset{k_d}{\overset{k_a}{\rightleftarrows}} P_i^*$
Chain growth	$P_i^* + M \overset{k_p}{\rightarrow} P_{i+1}$
Chain Transfer	
To monomer	$P_i + M \overset{k_m}{\rightarrow} \Lambda_i + P_1$
To solvent	$P_i + S \overset{k_s}{\rightarrow} \Lambda_i + P_1$
Termination:	
Unimolecular	$P_1 \overset{k_t}{\rightarrow} \Lambda_i$

Table II Kinetic Constant Ratios Estimated by Freitas[24] (R = 8.314 J/(mol*K)

Kinetic Constant Ratio	Homogeneous Polymerization	Heterogeneous Polymerization
$\frac{k_d}{k_p}$ (mol/ℓ)	$29.768 \exp\left(\frac{-5163}{RT}\right)$	negligible
$\frac{k_m}{k_a}$ (ℓ/mol)	$0.0142 \exp\left(\frac{-9736}{RT}\right)$	$0.00404 \exp\left(\frac{-8605}{RT}\right)$
$\frac{k_s}{k_a}$ (ℓ/mol)	$0.0102 \exp\left(\frac{-13593}{RT}\right)$	$2287 \exp\left(\frac{-34969}{RT}\right)$
$\frac{k_t}{k_a}$	$0.3153 \exp\left(\frac{-14483}{RT}\right)$	$4.01*10^{-7} \exp\left(\frac{2526}{RT}\right)$

chloride, Kennedy and Thomas[18] assumed that the deactivation step could be neglected in methyl chloride medium, so that the ionic growing chain would always be activated and ready to propagate. Freitas[24] assumed that the heterogeneous polymerization proceeds in a continuous monomer solution, where the polymer phase is suspended. These assumptions are supported by results presented by Kennedy, Kirshenbaum, and Thomas,[19] which show that chain addition is extremely fast and does not depend on monomer concentration. Freitas[24] also assumed that both polymer-rich and monomer-rich phases are in thermodynamic equilibrium, which is attained due to the large difference between average reactor residence time and reaction time. Finally, it has been assumed that reaction rates are not limited by diffusion.

The lifetime of the polyisobutylene growing chains are very small,[17] and quasi steady-state approximation can be applied for the growing chains.

Isobutylene polymerizations are extremely fast,[2,14-16] so that the polymerization is over in a few seconds in batch systems.[15] For this reason, it is not possible to follow the kinetics of polymerization and to determine the kinetic constants independently. Kennedy and co-workers[17-20,23] determined the ratios of some kinetic constants from molecular weight data, but they did not consider the termination step in the kinetic mechanism. Later, Kennedy and Squires[21] showed that espontaneous unimolecular termination occurs but did not reevaluate the kinetic constant ratios. As monomer conversion is not complete in batch systems,[15,18] Freitas reevaluated the kinetic ratios based on conversion and molecular weight data presented by Kennedy and coworkers.[15,18-20,23] These kinetic ratios are presented in Table II.

REACTOR MODELS

Solution Polymerization Reactor

A schematic diagram of the solution isobutylene homopolymerization rector is shown in Figure 1.

Polymerization occurs in a constant volume, jacketed-stirred tank reactor. The solvent is n-pentane and the reaction mechanism is the one presented before. As the density of the mixture is not constant, inlet and outlet volumetric flow rates are different. In the industrial reactor the monomer and catalyst feed streams are admitted at the same reactor position,[26] so that a single global feed stream, composed hypothetically of solvent, monomer, and catalyst, is fed to the reactor. As the catalyst feed rate is much lower than the monomer and solvent feed rates, its contribution to feed composition is negligible.

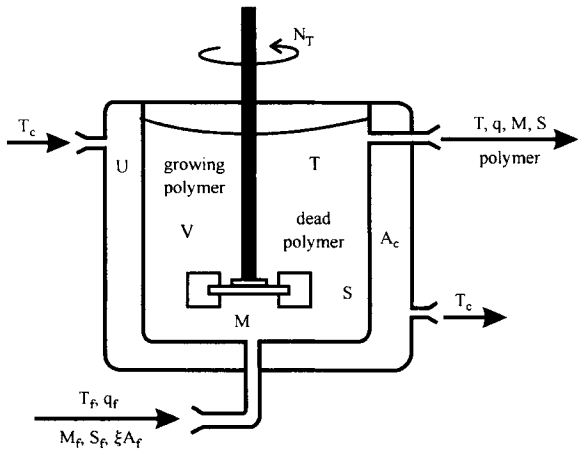

Figure 1 Schematic diagram of a solution isobutylene polymerization reactor.

It is important to emphasize that heat transfer at many industrial reactors is usually much more complex than described here. However, as shown by Athey,[27] heat exchangers where boiling or condensing fluids are used may present very complex behavior by themselves and may lead the whole reaction equipment to unstable conditions. The same may be said about autorefrigerated reactors, where condensers are used to remove the heat of reaction.[28] For this reason, the heat removal mechanism has been kept as simple as possible, in order to allow the analysis of the natural dynamic behavior introduced by the reaction mechanism only.

Then the solution isobutylene homopolymerization reactor model may be described by the following set of differential-algebraic equations:

$$V\frac{dM}{dt} = M_f q_f - Mq - \left[1 + \frac{k_a k_p M}{k_t(k_d + k_p M)} + \frac{k_m M}{k_t}\right]\xi A_f q_f \quad (1)$$

$$V\frac{dS}{dt} = S_f q_f - Sq - \left[\frac{k_s S}{k_t}\right]\xi A_f q_f \quad (2)$$

$$V\frac{d\rho}{dt} = \rho_f q_f - \rho q \quad (3)$$

$$\rho cpV\frac{dT}{dt} = \rho_f cp_f q_f(T_f - T) + (-\Delta H_p)\left[1 + \frac{k_a k_p M}{k_t(k_d + k_p M)} + \frac{k_m M}{k_t}\right]\xi A_f q_f + UA_c(T_c - T) \quad (4)$$

where M is the monomer concentration; M_f is the monomer feed concentration; V is the reactor volume; S is the solvent concentration; S_f is the solvent feed concentration; T is the reactor temperature; ρ is the density of the reactive mixture; ρ_f is the density of the feed stream; A_f is the $AlCl_3$ feed concentration; ξ is the catalyst efficiency; ξA_f is the initiator feed concentration; $(-\Delta H_p)$ is the heat of polymerization; q_f is the volumetric feed flow rate; q is the outlet volumetric flow rate; U is the global heat transfer coefficient; A_c is the effective heat transfer area; T_c is the coolant temperature; T_f is the feed temperature; cp is the specific heat of the reactive mixture; cp_f is the specific heat of the feed stream. Here, the heat transfer coefficient is a function of fluid viscosity, which is a function of mixture composition, temperature, and polymer molecular weight. Shaft work has been neglected. Monomer and solvent feed concentrations can be written as:

$$M_f = \frac{\rho_{M,f}}{M_M}\nu_{M,f} \quad (5)$$

$$S_f = \frac{\rho_{s,f}}{M_s}(1 - \nu_{M,f}) \quad (6)$$

where $\nu_{M,f}$ is the monomer feed volume fraction; M_M is the monomer molecular weight; M_S is the solvent molecular weight; $\rho_{M,f}$ and $\rho_{S,f}$ are the monomer and solvent densities at feed temperature.

The model equations can be rewritten as:

$$\frac{dM}{dt} = \frac{\nu_{M,f}}{\theta_f}\frac{\rho_{M,f}}{M_M} - \frac{M}{\theta} - \left[1 + \frac{k_a k_p M}{k_t(k_d + k_p M)} + \frac{k_m M}{k_t}\right]\frac{\xi A_f}{\theta_f} \quad (7)$$

$$\frac{dS}{dt} = \frac{(1 - \nu_{M,f})}{\theta_f}\frac{\rho_{s,f}}{M_s}\frac{S}{\theta} - \left[\frac{k_s S}{k_t}\right]\frac{\xi A_f}{\theta_f} \quad (8)$$

$$\frac{d\rho}{dt} = \left[\left(\frac{\partial\rho}{\partial T}\right)\frac{dT}{dt} + \left(\frac{\partial\rho}{\partial M}\right)\frac{dM}{dt} + \left(\frac{\partial\rho}{\partial S}\right)\frac{dS}{dt}\right] = \frac{\rho_f}{\theta_f} - \frac{\rho}{\theta} \quad (9)$$

$$\frac{dT}{dt} = \frac{\rho_f cp_f(T_f - T)}{\rho cp\theta_f} + \frac{(-\Delta H_P)}{\rho cp}\left[1 + \frac{k_a k_p M}{k_t(k_d + k_p M)} + \frac{k_m M}{k_t}\right]\frac{\xi A_f}{\theta_f} + \frac{UA_c}{\rho cpV}(T_c - T) \quad (10)$$

where $\theta_f = V/q_f$ is the reactor charging time and $\theta = V/q$ is the reactor discharging time. In order to describe the polymer molecular weight distribution, the moments of molecular weight distribution can be written as:

$$\frac{d\lambda_0}{dt} = \left[\frac{k_m M + k_s S + k_t}{k_t}\right]\frac{\xi A_f}{\theta_f} - \frac{\lambda_0}{\theta} \quad (11)$$

$$\frac{d\lambda_1}{dt} = \left[\frac{k_m M + k_s S + k_t}{k_t}\right]\frac{\xi A_f}{(1 - \alpha)\theta_f} - \frac{\lambda_1}{\theta} \quad (12)$$

$$\frac{d\lambda_2}{dt} = \left[\frac{k_m M + k_s S + k_t}{k_t}\right]\frac{(1 + \alpha)\xi A_f}{(1 - \alpha)^2\theta_f} - \frac{\lambda_2}{\theta} \quad (13)$$

where λ_0, λ_1, λ_2, are, respectively, the zeroth, first, and second moments of dead polymer molecular weight distribution. α is the propagation probability defined as:

$$\alpha = \frac{\dfrac{k_a k_p M}{k_d + k_p M}}{\dfrac{k_a k_p M}{k_d + k_p M} + k_m M + k_s S + k_t} \quad (14)$$

As concentration of growing chains is much lower than the concentration of dead chains, their contribution to the overall molecular weight is assumed to be negligible. The number average degree of polymerization is:

$$DP \equiv \frac{\lambda_1}{\lambda_0} \quad (15)$$

The number average and weight average molecular weights are:

$$\bar{M}_n \equiv M_M \frac{\lambda_1}{\lambda_0} \quad (16)$$

$$\bar{M}_w \equiv M_m \frac{\lambda_2}{\lambda_1} \quad (17)$$

The polydispersity index is:

$$Q \equiv \frac{\bar{M}_w}{\bar{M}_n} = \frac{\lambda_2 \lambda_0}{\lambda_1^2} \quad (18)$$

Monomer conversion is:

$$\chi = \frac{\lambda_1}{\lambda_1 + M} \quad (19)$$

According to Brandrup and Imergutt,[29] the heat of isobutylene polymerization is 963 kJ/kg of the polymer. If the thermal resistance of the reactor wall is negligible, the overall heat transfer coefficient, U, is given by:

$$\frac{1}{U} = \frac{1}{h_i} + \frac{1}{h_o} \quad (20)$$

where h_i and h_o are the inside and the outside film heat transfer coefficients of the reactor, respectively. The outside heat transfer coefficient (h_o) is assumed to be constant and equal to 1420W/m^2/K, a minimum design value for jacketed reactors,[30,31] and the inside film heat transfer coefficient (h_i) is estimated from the Chapman[32] correlation, suggested for a standard jacketed reactor[31]:

$$\frac{h_i \cdot D_r}{k} = 0.73 \mathrm{Re}^{0.65} \mathrm{Pr}^{0.33} \left(\frac{\eta}{\eta_w}\right)^{0.24} \quad (21)$$

where D_r is the reactor diameter, k is the thermal conductivity of the reacting mixture, η is the viscosity of the reacting mixture,η_w is the fluid viscosity at the wall temperature, Re is the Reynolds number, and Pr is the Prandlt number defined as:

$$\mathrm{Re} = \frac{\rho D_T^2 N_T}{\eta} \quad (22a)$$

$$\mathrm{Pr} = \frac{\eta c p}{k} \quad (22b)$$

where D_T is the turbine impeller diameter and N_T is the rotational speed of the turbine impeller. The dimensions of the solution reactor are presented in Table III.

The viscosity of the polymer solution is given by the Huggins equation:[29,33]

$$\eta = \eta_0 (1 + \eta_{sp}) \quad (23a)$$

$$\eta_{sp} = [\eta] C_{pol} (1 + 0.4 [\eta] C_{pol}) \quad (23b)$$

where η_{sp} is the Huggins specific viscosity; η_0 is the viscosity of the isobutylene–n-pentane mixture; $[\eta]$ is the Mark–Houwink intrinsic viscosity, and C_{pol} is the polymer weight concentration. The viscosity of the isobutylene–n-pentane mixture is an average of the monomer and solvent viscosities, given by Reid, Prausnitz, and Poling:[34]

$$\ln(\eta_M(T)) = -6.447 + 813.5/T + 0.0132T - 2.438E - 5{*}T^2 \quad (24)$$

$$\ln(\eta_S(T)) = -3.958 + 722.2/T \quad (25)$$

The intrinsic viscosity is given by the Mark–Houwink equation:

$$[\eta] = 1.73{*}10^{-5} \bar{M}_w^{0.70} \quad (26)$$

where the coefficients were estimated in accordance to Van Krevelen and Hoftyzer.[29,33]

Then the viscosity of the polymer solution and

Table III Solution Reactor Geometry

Parameter	Value
Reactor diameter (m)	2.90
Reactor volume (l)	18927
Impeller diameter (m)	0.967
Heat transfer area (m^2)	31.30
Impeller velocity (rpm)	60.0

Table IV Physical Constants of Individual Chemical Species[24,33–37]

Property	Density, ρ, (kg/l)	Specific Heat, cp, (kJ/kg/K)	Thermal Conductivity, k, (W/m/K)	Molecular Weight, M (g/mol)
Isobutylene	0.901–1.01E-4*T	1.890	0.224–4.24E-4*T	56.108
n-Pentane	0.886–8.72E-4*T	1.982	0.209–3.0E-4*T	72.15
Methyl chloride	1.378–1.52E-3*T	1.473	0.378–6.6E-3*T	50.49
Polymer	1.01–5.06E-4*T	1.479	0.134	—

the heat transfer coefficient depend on isobutylene concentration, n-pentane concentration, polymer concentration, temperature, and on the first and second moments of the molecular weight distribution.

The specific heat and thermal conductivity of the reactive mixture are obtained as:

$$k = \sum_{j=M,S,P} \omega_j k_j(T) \tag{27}$$

$$cp = \sum_{j=M,SP} \omega_j cp_j \tag{28}$$

where ω_j is the mass fraction of species j. The density of the reactive mixture is given by:

$$\rho = \sum_{j=M,S,P} \nu_j \rho_j(T)$$

$$= \rho_P + (\rho_M - \rho_P)\nu_M + (\rho_S - \rho_P)\nu_S \tag{29}$$

where ν_j is the volume fraction of species j. The physical constants of the individual chemical species are shown in Table IV.

If the heat transfer coefficient is constant, the reactor model can be divided into two subsystems, where the first subsystem [eqs. (7)–(10)] is independent of the second subsystem [eqs. (11)–(13)]. In such a case, the reactor dynamics can be studied by analyzing only the first subsystem. In the reactor model just described, the heat transfer coefficient is a function of isobutylene concentration, n-pentane concentration, polymer concentration, temperature, and the first and second moments of the molecular weight distribution. Thus, the system dynamics also depends on the first and second moments of the molecular weight distribution [eqs. (12)–(13)].

Precipitation Polymerization Reactor

A schematic diagram of the heterogeneous isobutylene homopolymerization rector is shown in Figure 2.

As already discussed, the mechanism of the heterogeneous isobutylene polymerization is similar to the mechanism of the homogeneous polymerization. Reactions take place in the continuous phase, producing dead polymer, which precipitates and forms a nonreactive disperse phase. The dead polymer concentration in the continuous phase is assumed to be negligible. Both monomer-rich and polymer-rich phases are assumed to be in thermodynamic equilibrium. Reactor volume is assumed to be constant and the quasi steady-state hypothesis is used to describe the growing chains. The reactor is assumed to be perfectly mixed.

Then the dynamic reactor model may be described by the following system of differential-algebraic equations:

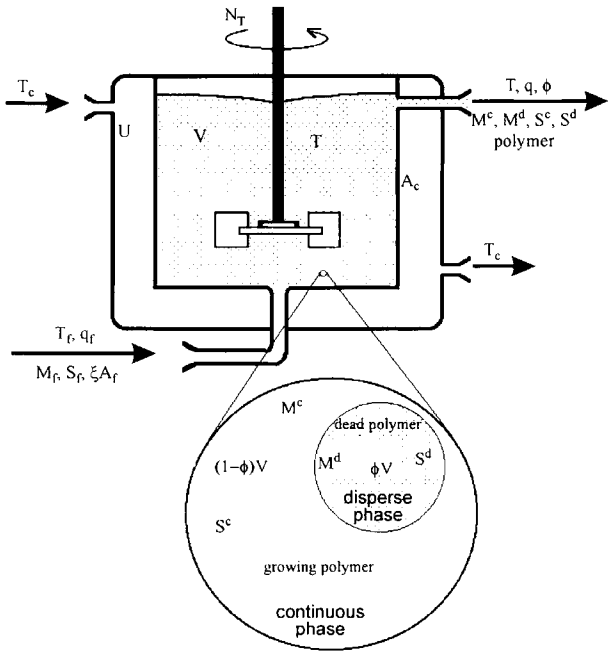

Figure 2 Schematic diagram of a precipitation isobutylene polymerization reactor

$$V\frac{d[M^c(1-\phi)+M^d\phi]}{dt} = M_f q_f - [M^c(1-\phi)+M^d\phi]q - \Re_M V \quad (30)$$

$$V\frac{d[S^c(1-\phi)+S^d\phi]}{dt} = S_f q_f - [S^c(1-\phi)+S^d\phi]q - \Re_S V \quad (31)$$

$$V\frac{d[\phi\rho_P\nu_P^d]}{dt} = -q\phi\rho_P\nu_P^d + (M_M\Re_M + M_S\Re_S)V \quad (32)$$

$$\rho c_P V\frac{dT}{dt} = \rho_f c_{Pf} q(T_f - T) + (-\Delta H_P)(M_M\Re_M + M_S\Re_S)V + UA_c(T_c - T) \quad (33)$$

$$\Re_M = \frac{\xi A_f}{\theta_f}\left[1 + \frac{k_a}{k_t} + \frac{k_m M^c}{k_t}\right] \quad (34)$$

$$\Re_S = \frac{\xi A_f}{\theta_f}\left[\frac{k_s S^c}{k_t}\right] \quad (35)$$

where M^c is the monomer concentration in the continuous phase; M^d is the monomer concentration in the disperse phase; M_f is the monomer feed concentration; V is the reactor volume; ϕ is the volume fraction of the disperse phase; S^c is the solvent concentration in the continuous phase; S^d is the solvent concentration in the disperse phase; S_f is the solvent feed concentration; T is the reactor temperature; ρ is the density of the reactive mixture; ρ_f is the density of the feed stream; A_f is the $AlCl_3$ feed concentration; ξ is the catalyst efficiency and ξA_f is the initiator feed concentration; $(-\Delta H_p)$ is the heat of polymerization; q_f is the volumetric feed flow rate; q is the volumetric outlet flow rate; U is the global heat transfer coefficient; A_c is the effective heat transfer area; T_c is the coolant temperature; T_f is the feed temperature; cp is the specific heat of the reactive mixture; cp_f is the specific heat of the feed stream. Shaft work has been neglected. Reactor dimensions are presented in Table V.

It is assumed that the Flory–Huggins equation[29,33,38] may be used to describe the thermodynamic equilibrium as:

$$\sum_i \nu_i^d = \nu_M^d + \nu_S^d + \nu_P^d = 1 \quad (36)$$

$$x_M^c = \nu_M^d \exp(\nu_P^d + \chi_M(\nu_P^d)^2) \quad (37)$$

$$x_s^c = (1 - x_M^c) = \nu_s^d \exp(\nu_P^d + \chi_S(\nu_P^d)^2) \quad (38)$$

Table V Precipitation Reactor Geometry

Parameter	Value
Reactor diameter (m)	2.90
Reactor volume (l)	18927
Impeller diameter (m)	0.967
Heat transfer area (m^2)	31.30
Impeller velocity (rpm)	600.0

where ν_M^d, ν_s^d, and ν_P^d, are the monomer, solvent, and polymer volume fractions in the disperse phase, $x^c{}_M$ and $x^c{}_s$ are the monomer and solvent molar fractions in the continuous phase, and χ_i are the Flory–Huggins interaction parameters. Based on literature data,[29,33,38] Freitas[24] estimated the isobutylene–polyisobutylene and methyl chloride–polyisobutylene Flory–Huggins interaction parameters as:

$$\chi_M = 0.249 + 17.3/T \quad (39)$$

$$\chi_S = -1.631 + 706/T \quad (40)$$

Equations (36)–(38) can be combined as:

$$h(\nu_P^d, T, \nu_M^c) = \frac{M_S\rho_M\nu_M^c\exp(-\nu_P^d - \chi_M(T)(\nu_P^d)^2)}{[M_M\rho_S(1-\nu_M^c) + M_S\rho_M\nu_M^c]} + \frac{M_M\rho_S(1-\nu_M^c)\exp(-\nu_P^d - \chi_S(T)(\nu_P^d)^2)}{[M_M\rho_S(1-\nu_M^c) + M_S\rho_M\nu_M^c]} + \nu_P^d - 1 = 0 \quad (41)$$

According to Kresge,[1] the heat of polymerization in precipitation processes is 820 kJ/kg of the polymer. This value is different from the one presented previously, probably due to the heat effects associated with the polymer precipitation in the strongly nonideal solution.

The moments of the molecular weight distribution may be described as:

$$V\frac{d[\phi\lambda_0]}{dt} = \left[\frac{k_m M^c + k_s S^c + k_t}{k_t}\right]\xi A_f q_f - \lambda_0\phi q \quad (42)$$

$$V\frac{d[\phi\lambda_1]}{dt} = \left[\frac{k_m M^c + k_s S^c + k_t}{k_t}\right]\frac{\xi A_f q_f}{(1-\alpha)} - \lambda_1\phi q \quad (43)$$

$$V\frac{d[\phi\lambda_2]}{dt} = \left[\frac{k_m M^c + k_s S^c + k_t}{k_t}\right] \times \frac{(1+\alpha)}{(1-\alpha)^2}\xi A_f q_f - \lambda_2\phi q \quad (44)$$

where α is the propagation probability defined by:

$$\alpha = \frac{k_a}{k_a + k_m M^c + k_s S^c + k_t} \quad (45)$$

The overall heat transfer coefficient of the reactor, U, is given by eq. (20). The outside heat transfer coefficient (h_o) is assumed to be constant and equal to 1420 W/m^2/K. The inside film heat transfer coefficient (h_i) is obtained from the Frantisak[39] correlation, developed for solid–liquid suspensions in standard jacketed reactors:[31]

$$\frac{h_i \cdot D}{k} = 0.575\mathrm{Re}^{0.60}\mathrm{Pr}^{0.26}\left(\frac{D}{D_T}\right)^{0.33} \times \left(\frac{cp^d}{cp^c}\right)^{0.13}\left(\frac{\rho^d}{\rho^c}\right)^{-0.16}\left(\frac{\phi}{1-\phi}\right)^{-0.04} \quad (46)$$

where the Reynolds number and Prandlt number are defined by eq. (22). Suspension viscosity depends on temperature, particle volume fraction, particle shape and size, and on the viscosity of the continuous phase. According to Frantisak and coworkers,[39] suspension viscosity can be related to particle volume fraction and viscosity of the continuous phase as:

$$\eta_r = \frac{\eta}{\eta^c} = 1 + 2.5\phi + 7.54\phi^2 \quad (47)$$

where η^c is the viscosity of the continuous phase, obtained as an average of isobutylene [eq. (24)] and methyl chloride viscosities.[34] The methyl chloride viscosity is given by Reid, Prausnitz, and Poling:[34]

$$\ln(\eta_S(T)) = -5.07 + 981.9/T \quad (48)$$

The thermal conductivity of the suspension is given by the Maxwell equation:[39]

$$k = k^c \frac{2k^c + k^d - 2\phi(k^c - k^d)}{2k^c + k^d + \phi(k^c - k^d)} \quad (49)$$

where k is the thermal conductivity of the suspension, k^d is the thermal conductivity of the disperse phase, and k^c is the thermal conductivity of the continuous phase. Individual phase thermal conductivities were calculated as described by eq. (27). Suspension density is given by:

$$\rho = \phi\rho^d + (1-\phi)\rho^c \quad (50)$$

Individual phase densities are given by eq. (29). Suspension and individual phase specific heats are weight averages of the specific heats of the components. Physical properties of isobutylene and methyl chloride are shown in Table IV. As viscosity and other physical properties do not depend on polymer molecular weight, the dynamics of precipitation reactors can be analyzed by using only the mass and energy balances. Using eq. (41), mass and energy balances [eqs. (30)–(33)] can be rewritten as functions of a smaller set of state variables:

$$\frac{d[\rho_M[\nu_M^c(1-\phi) + \nu_M^d\phi]]}{dt} = \frac{\nu_{M,f}}{\theta_f}\rho_{M,f} - \frac{\rho_M[\nu_M^c(1-\phi) + \nu_M^d\phi]}{\theta} - \boldsymbol{R}_M \quad (51)$$

$$\frac{d[\rho_S[(1-\nu_M^c)(1-\phi) + \nu_s^d\phi]]}{dt} = \frac{\nu_{s,f}}{\theta_f}\rho_{s,f} - \frac{\rho_S[(1-\nu_M^c)(1-\phi) + \nu_S^d\phi]}{\theta} - \boldsymbol{R}_S \quad (52)$$

$$\frac{d[\phi\rho_P\nu_P^d]}{dt} = -\frac{\phi\rho_P\nu_P^d}{\theta} + \boldsymbol{R}_M + \boldsymbol{R}_S \quad (53)$$

$$\frac{dT}{dt} = \frac{\rho_f cp_f(T_f - T)}{\rho cp\theta_f} + \frac{(-\Delta H_P)}{\rho cp}(\boldsymbol{R}_M + \boldsymbol{R}_S) + \frac{UA_c}{\rho cpV}(T_c - T) \quad (54)$$

where $\boldsymbol{R}_M$ and $\boldsymbol{R}_S$ are monomer and solvent reaction rates:

$$\boldsymbol{R}_M = M_M\frac{\xi A_f}{\theta_f}\left[1 + \frac{k_a}{k_t} + \frac{k_m}{k_t}\left(\frac{\nu_M^c\rho_M}{M_M}\right)\right] \quad (55)$$

$$\boldsymbol{R}_S = \frac{\xi A_f}{\theta_f}\frac{k_s}{k_t}\rho_s(1-\nu_M^c) \quad (56)$$

As ν_M^d, ν_s^d are functions of ν_P^d, T, and ν_M^c, the structure of the system formed by eqs. (51)–(54) is:

$$\frac{d\underline{f}(\nu_M^c, \phi, T, \nu_P^d)}{dt} = \underline{g}(\nu_M^c, \phi, T, \nu_P^d, \theta) \quad (57)$$

Equations (41) and (51)–(54) describe the dynamics of the precipitation reactor.

STEADY-STATE AND DYNAMIC ANALYSIS

Solution Reactor Dynamics

The solution reactor model [eqs. (7)–(10), (12), and (13)], was solved by using 4th and 5th-order Runge–Kutta Fehlberg methods.[40] Nominal operation conditions for the solution reactor are presented in Table VI.

Figure 3 shows the open loop temperature response to step changes in the feed temperature. The system is initially at steady-state conditions. The feed temperature is then changed from an initial value of 173.15 K to 163.15 K, to 173.15 K, to 183.15 K, and back to 173.15 K at intervals of 10 h.

Figure 3 indicates that the steady states obtained at feed temperatures of 163.15 K, 173.15 K, and 183.15 K are stable and that process dynamics is nearly linear. The system attains new steady-state conditions after roughly 5 h. Figure 4 shows the degree of polymerization, conversion, polydispersity, and viscosity responses to feed temperature perturbations.

It may be seen in Figure 4 that an increase (decrease) of reactor temperature leads to a decrease (increase) of both the degree of polymerization and the viscosity of the polymer solution. Consequently, heat transfer rate increases (decreases) and pulls the reactor temperature down (up). This dumping mechanism stabilizes the overall reactor operation.

Solution Reactor Steady-State Performance

At steady state, the solution reactor model may be written as:

$$\frac{\nu_{M,f}}{\theta_f}\frac{\rho_{M,f}}{M_M} - \frac{M}{\theta} - \left[1 + \frac{k_a k_p M}{k_t(k_d + k_p M)} + \frac{k_m M}{k_t}\right]\frac{\xi A_f}{\theta_f} = 0 \quad (58)$$

Table VI Nominal Operation Conditions for the Solution Polymerization Reactor

Operation Conditions	Initial Steady State
T_f = 173.15 K	M = 2.23 mol/L
(manipulated variable)	S = 8.09 mol/L
T_c = 173.15 K	T = 183.35 K
ϕ_f = 2.0 h	$\lambda_0 = 3.7 \times 10^{-5}$
$\xi A_f = 10^{-5}$ mol/L	λ_1 = 0.292
$\nu_{M,f}$ = 0.20	λ_2 = 4564.5

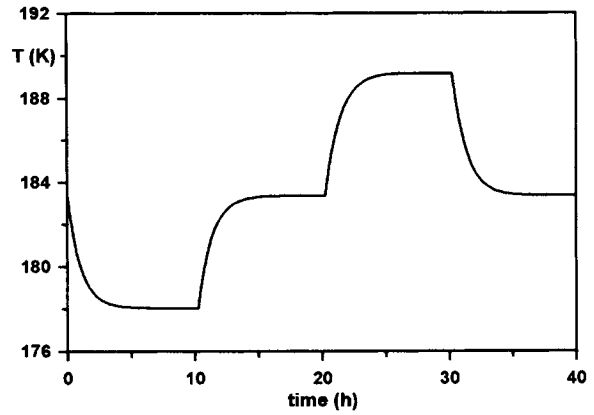

Figure 3 Open loop temperature response to feed temperature step changes. Solution reactor. Operation conditions: $\nu_{M,f}$ = 0.20, T_c = 173 K, $\xi A_f = 10^{-5}$ mol/L.

$$\frac{(1-\nu_{M,f})}{\theta_f}\frac{\rho_{s,f}}{M_S} - \frac{S}{\theta} - \left[\frac{k_s S}{k_t}\right]\frac{\xi A_f}{\theta_f} = 0 \quad (59)$$

$$\frac{\rho_f c p_f (T_f - T)}{\rho c p \theta_f} + \frac{(-\Delta H_P)}{\rho c p}\left[1 + \frac{k_a k_p M}{k_t(k_d + k_p M)} + \frac{k_m M}{k_t}\right]\frac{\xi A_f}{\theta_f} + \frac{UA_c}{\rho c p V}(T_c - T) = 0 \quad (60)$$

$$\theta = \frac{\rho}{\rho_f}\theta_f \quad (61)$$

$$\left[\frac{k_m M + k_s S + k_t}{k_t}\right]\frac{\xi A_f}{\theta_f} - \frac{\lambda_0}{\theta} = 0 \quad (62)$$

$$\left[\frac{k_m M + k_s S + k_t}{k_t}\right]\frac{\xi A_f}{(1-\alpha)\theta_f} - \frac{\lambda_1}{\theta} = 0 \quad (63)$$

$$\left[\frac{k_m M + k_s S + k_t}{k_t}\right]\frac{(1+\alpha)\xi A_f}{(1-\alpha)^2\theta_f} - \frac{\lambda_2}{\theta} = 0 \quad (64)$$

So that:

$$GP = \frac{\lambda_1}{\lambda_0} = \frac{1}{(1-\alpha)} \quad (65)$$

$$\bar{M}_n \equiv M_M\frac{\lambda_1}{\lambda_0} = \frac{M_M}{(1-\alpha)} \quad (66)$$

$$\bar{M}_w \equiv M_M\frac{\lambda_2}{\lambda_1} = \frac{(1+\alpha)}{(1-\alpha)}M_M \quad (67)$$

$$Q \equiv \frac{\bar{M}_w}{M_n} = \frac{\lambda_0\lambda_2}{\lambda_1^2} = 1 + \alpha \quad (68)$$

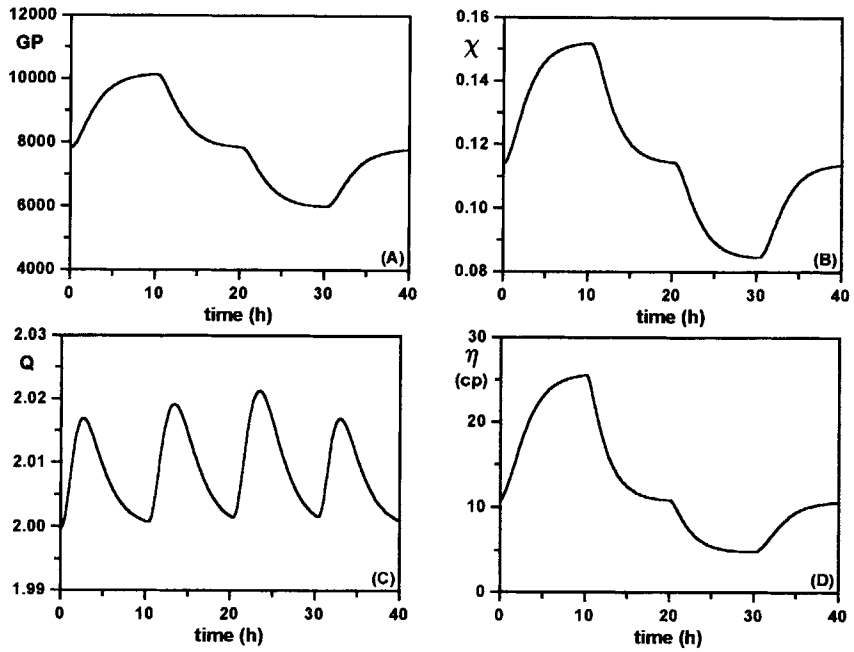

Figure 4 Dynamic response of polymer properties to feed temperature perturbations. Solution reactor. Operation conditions: $\nu_{M,f} = 0.20$, $T_c = 173$ K, $\xi A_f = 10^{-5}$ mol/L.

As the degree of polymerization is large, the propagation probability is close to 1 and the polyisobutylene polydispersity is close to 2, which was observed in all reactor simulations.

Rearranging model equations, it is possible to write:

$$\frac{\nu_{M,f}\rho_{M,f}}{M_M} - \frac{\rho_f}{\rho} M - \left[1 + \frac{k_a k_p M}{k_t(k_d + k_p M)} + \frac{k_m M}{k_t}\right] \xi A_f = 0 \quad (69)$$

$$\frac{(1 - \nu_{M,f})\rho_{s,f}}{M_s} - \frac{\rho_f}{\rho} S - \left[\frac{k_s S}{k_t}\right] \xi A_f = 0 \quad (70)$$

$$T_f - T + \frac{(-\Delta H_P)}{\rho_f c p_f}\left[1 + \frac{k_a k_p M}{k_t(k_d + k_p M)} + \frac{k_m M}{k_t}\right] \xi A_f + \frac{UA_c}{\rho_f c p_f V}(T_c - T)\theta_f = 0 \quad (71)$$

From eq. (71) one can see that, when the charging time is equal to zero, the reactor is operated adiabatically. In this case, reactor temperature is given by:

$$T_a = T_f + \frac{(-\Delta H_P)}{\rho_f c p_f} \times \left[1 + \frac{k_a k_p M}{k_t(k_d + k_p M)} + \frac{k_m M}{k_t}\right] \xi A_f \quad (72)$$

One can also see that, if the charging time becomes very large, the reactor temperature tends to the coolant temperature. If the coolant temperature is equal to the adiabatic temperature, then steady-state reactor temperature is always equal to the adiabatic temperature and does not depend on the charging time.

The system formed by eqs. (69)-(71) was solved with a continuation method,[40,41] where charging time was the continuation parameter. Stability calculations were carried out simultaneously, based on the First Method of Liapunov,[44] which means that the eigenvalues of the Jacobian matrix of the DAE system formed by eqs. (7)-(10), (12), and (13) were obtained (Press and co-workers QR code[42]) and analyzed (see Appendix). In all cases analyzed, the eingenvalues were real and strictly negative, which means that the reactor is stable, does not oscillate, and does not present steady-state multiplicity. The real parts of the eingenvalue spectra are shown in Figure 5 as functions of charging time.

Figure 6 shows steady-state reactor temperatures for different coolant temperatures. Reactor temperature always increases or decreases monotonously, between adiabatic temperature and coolant temperature. When the coolant temperature is greater than the adiabatic temperature, the coolant fluid is used to heat the reactor, which is not of practical interest.

Reactor performance is influenced by temperature strongly. Figures 7 and 8 show the degree of

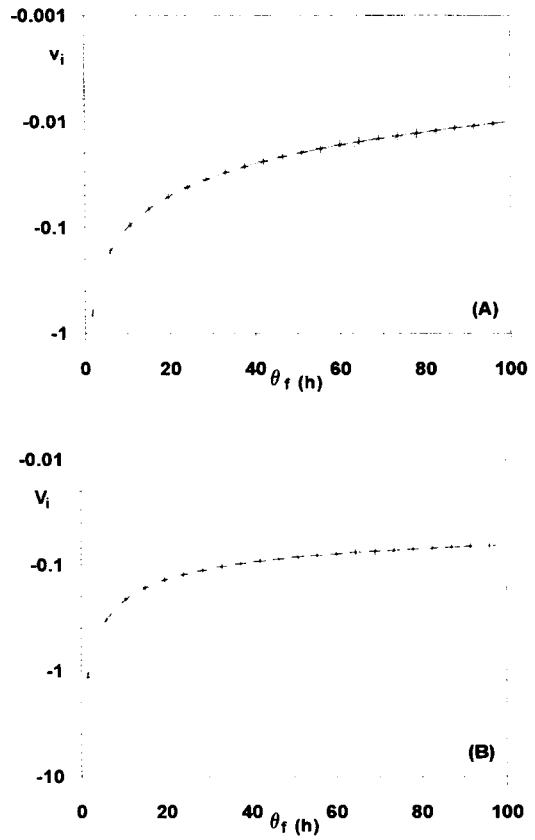

Figure 5 Eingenvalue spectra as functions of charging time. Solution reactor. (A) Smallest eingenvalue, (B) greatest eingenvalue. Operation conditions: $\nu_{M,f} = 0.20$, $T_f = 173$ K, $T_c = 173$ K, $\xi A_f = 10^{-5}$ mol/L.

polymerization and conversion as functions of the charging time. When compared to Figure 6, one can see that both the degree of polymerization and conversion decrease when reactor temperature increases. The degree of polymerization is a measure

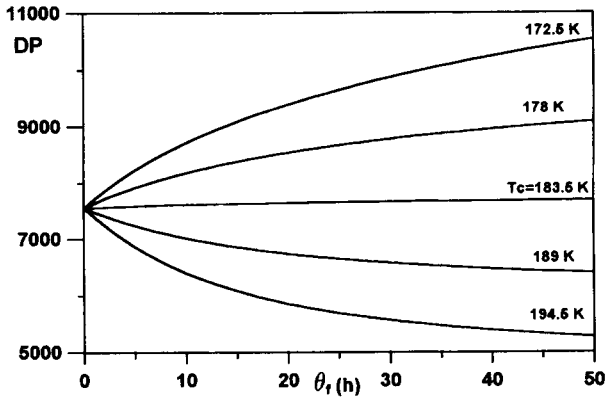

Figure 7 Degree of polymerization for various jacket temperatures. Solution reactor. Operation conditions: $\nu_{M,f} = 0.20$, $T_f = 173$ K, $\xi A_f = 10^{-5}$ mol/L.

of the competition between chain-growing (propagation step) and chain-breaking processes (chain transfer and termination steps). From Table II, the most important chain-breaking process is chain transfer to the monomer. As the difference between the activation energies of chain transfer to monomer and propagation is 14.90 kJ/mol, the rate of chain transfer grows faster than the rate of propagation as temperature increases, which means that larger degrees of polymerization should be expected at lower temperatures. Conversion depends mainly on the ratio between the rates of termination and propagation. From Table II, the difference between the activation energies of termination and propagation is 19.64 kJ/mol, which means that the rate of termination grows faster than the rate of propagation when temperature increases and that lower conversions should be expected at higher temperatures.

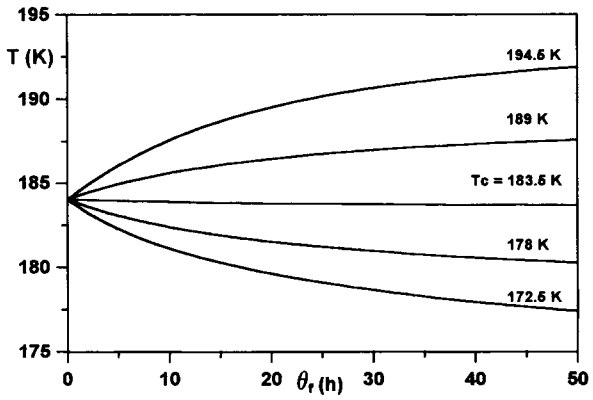

Figure 6 Steady-state reactor temperature as a function of jacket temperature. Solution reactor. Operation conditions: $\nu_{M,f} = 0.20$, $T_f = 173$ K, $\xi A_f = 10^{-5}$ mol/L.

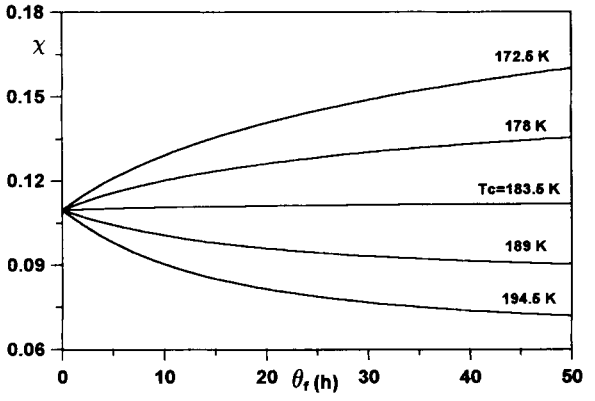

Figure 8 Conversion for various jacket temperatures. Solution reactor. Operation conditions: $\nu_{M,f} = 0.20$, $T_f = 173$ K, $\xi A_f = 10^{-5}$ mol/L.

Precipitation Reactor Steady-State Performance

At steady state conditions, the precipitation reactor model becomes:

$$\frac{M_S\rho_M\nu_M^c\exp(-\nu_P^d-\chi_M(T)(\nu_P^d)^2)}{[M_M\rho_S(1-\nu_M^c)+M_S\rho_M\nu_M^c]}+\frac{M_M\rho_S(1-\nu_M^c)\exp(-\nu_P^d-\chi_S(T)(\nu_P^d)^2)}{[M_M\rho_S(1-\nu_M^c)+M_S\rho_M\nu_M^c]}+\nu_P^d-1=0 \quad (41)$$

$$\frac{\nu_{M,f}}{\theta_f}\rho_{M,f}-\frac{\rho_M[\nu_M^c(1-\phi)+\nu_M^d\phi]}{\theta}-M_M\left[1+\frac{k_a}{k_t}+\frac{k_m}{k_t}\left(\frac{\nu_M^c\rho_M}{M_M}\right)\right]\frac{\xi A_f}{\theta_f}=0 \quad (73)$$

$$\frac{\nu_{s,f}}{\theta_f}\rho_{s,f}-\frac{\rho_S[(1-\nu_M^c)(1-\phi)+\nu_S^d\phi]}{\theta}-\frac{k_s}{k_t}\rho_S(1-\nu_M^c)\frac{\xi A_f}{\theta_f}=0 \quad (74)$$

$$-\frac{\phi\rho_P\nu_P^d}{\theta}+M_M\left[1+\frac{k_a}{k_t}+\frac{k_m}{k_t}\left(\frac{\nu_M^c\rho_M}{M_M}\right)\right]\frac{\xi A_f}{\theta_f}+\frac{k_s}{k_t}\rho_S(1-\nu_M^c)\frac{\xi A_f}{\theta_f}=0 \quad (75)$$

$$\frac{\rho_f cp_f(T_f-T)}{\rho cp\theta_f}+\frac{(-\Delta H_P)}{\rho cp}\left(M_M\left[1+\frac{k_a}{k_t}+\frac{k_m}{k_t}\left(\frac{\nu_M^c\rho_M}{M_M}\right)\right]+\frac{k_s}{k_t}\rho_S(1-\nu_M^c)\right)\frac{\xi A_f}{\theta_f}+\frac{UA_c}{\rho cpV}(T_c-T)=0 \quad (76)$$

$$\lambda_0=\left[\frac{k_m}{k_t}\left(\frac{\nu_M^c\rho_M}{M_M}\right)+\frac{k_s}{k_t}\frac{\rho_S}{M_S}(1-\nu_M^c)+1\right]\frac{\xi A_f}{\phi}\frac{\theta}{\theta_f} \quad (77)$$

$$\lambda_1=\frac{1}{(1-\alpha)}\left[\frac{k_m}{k_t}\left(\frac{\nu_M^c\rho_M}{M_M}\right)+\frac{k_s}{k_t}\frac{\rho_S}{M_S}(1-\nu_M^c)+1\right]\frac{\xi A_f}{\phi}\frac{\theta}{\theta_f} \quad (78)$$

$$\lambda_2=\frac{(1+\alpha)}{(1-\alpha)^2}\left[\frac{k_m}{k_t}\left(\frac{\nu_M^c\rho_M}{M_M}\right)+\frac{k_s}{k_t}\frac{\rho_S}{M_S}(1-\nu_M^c)+1\right]\frac{\xi A_f}{\phi}\frac{\theta}{\theta_f} \quad (79)$$

so that the degree of polymerization, number average, and weight average molecular weights and polydispersity may be described by the same equations presented before for the solution reactor [eqs. (65)-(68)]. Monomer conversion may be described as:

$$\chi=\frac{\phi\lambda_1}{\phi(\lambda_1+M^d)+(1-\phi)M^c} \quad (80)$$

As in the previous case, eqs. (41) and (73)–(76) were solved with a continuation method,[40,41] using charging time as the continuation parameter. The stability analysis was based on the First Method of Liapunov,[44] which means that the eigenvalues of the Jacobian matrix of the DAE system formed by eqs. (41), (73)–(76) were computed simultaneously with the steady-state solutions (see Appendix). As in the previous case, the eingenvalues were always real and strictly negative, which means that the precipitation reactor is also stable in the whole range

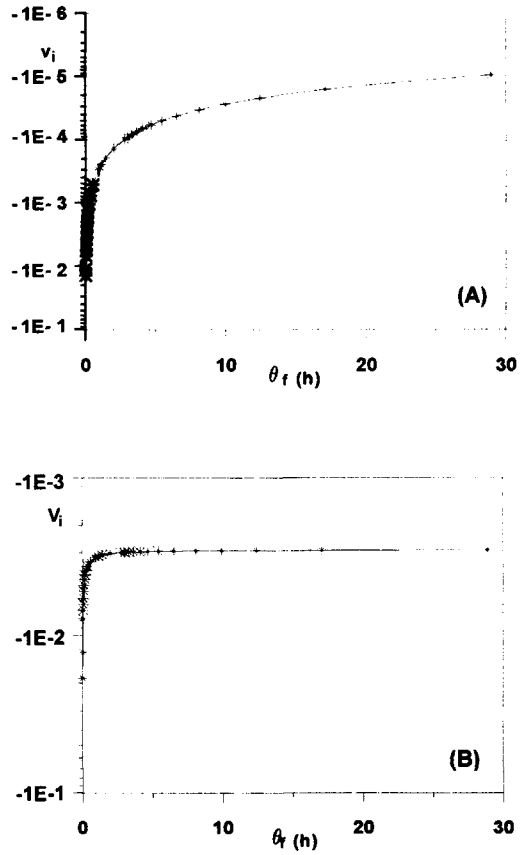

Figure 9 Eingenvalue spectra as a function of charging time. Precipitation reactor. (A) Smallest eingenvalue, (B) greatest eingenvalue. Operation conditions: $\xi A_f = 4 \times 10^{-6}$ mol/L, $\nu_{M,f} = 0.30$, $T_f = 173$ K.

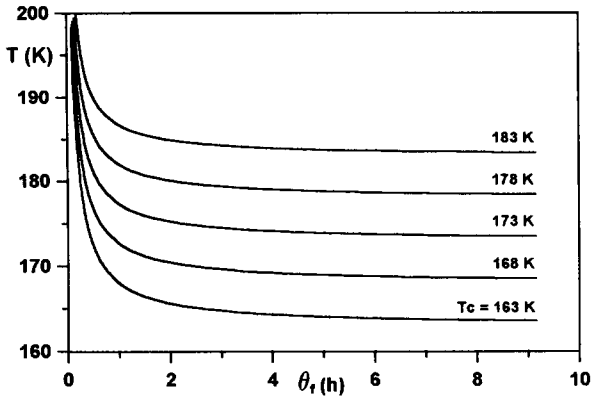

Figure 10 Steady-state reactor temperature as a function of jacket temperature. Precipitation reactor. Operation conditions: T_f = 173 K, $\nu_{M,f}$ = 0.30, A_f = 4 × 10^{-6} mol/L.

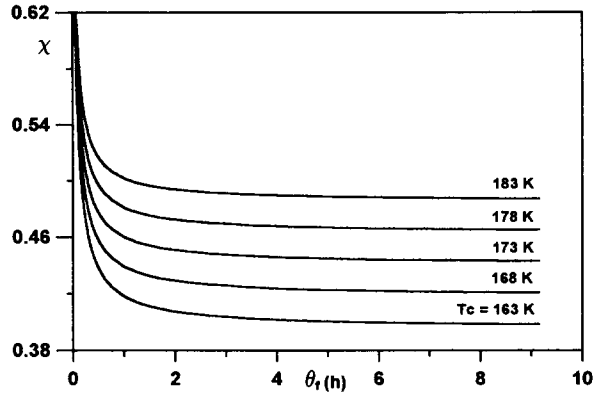

Figure 12 Coversion for various jacket temperatures. Precipitation reactor. Operation conditions: $\nu_{M,f}$ = 0.30, T_f = 173 K, A_f = 4 × 10^{-6} mol/L.

of operation conditions analyzed. So, the reactor does not oscillate and does not present steady-state multiplicity. The real parts of the eingenvalue spectra are shown in Figure 9 as a function of charging time.

The heterogeneous isobutylene polymerization reactor presents only one steady-state solution for each set of operation conditions. This is illustrated in Figure 10. As the solution reactor, two physical limits can be seen for reactor temperature in this system: the adiabatic temperature, for charging times close to zero, and the cooling jacket temperature, for very large charging times. As precipitation polymerization is more severe than solution polymerization, higher adiabatic temperatures and conversions are reached. Figures 11 and 12 show how the degree of polymerization and conversion change when both charging time and jacket temperature change. Comparing these figures with Figure 10, one can see that the degree of polymerization decreases and that conversion increases when temperature increases. It may be seen from Table II that the activation energy of the propagation step is larger than the activation energy of chain transfer to both monomer and solvent, which causes the decrease of the degree of polymerization as temperature increases. It may also be seen from Table II that the activation energy of the propagation step is larger than the activation energy of termination, which causes the increase of conversion as temperature increases. Dynamic simulations for the heterogeneous reactors are similar to the ones already presented for the homogeneous reactors and will not be shown here.

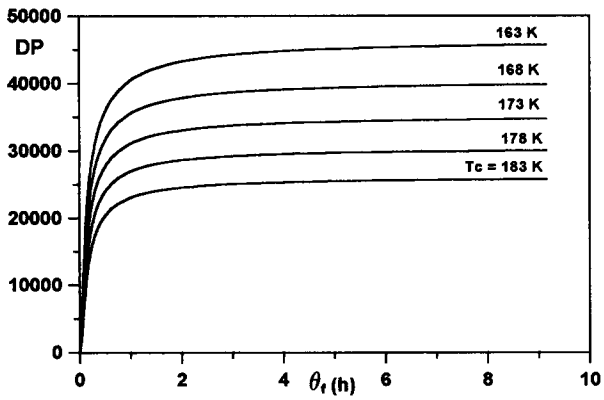

Figure 11 Degree of polymerization for various jacket temperatures. Precipitation reactor. Operation conditions: $\nu_{M,f}$ = 0.30, T_f = 173 K, A_f = 4 × 10^{-6} mol/L.

DISCUSSION

Figures 6–8 and 10–12 show that the steady-state responses of solution and precipitation reactors are significantly different. It is important to emphasize, though, that differences are mainly due to the different effective activation energies of the termination constants, as shown in Table II. While the solution termination reaction is thermally terminating, in the sense that termination increases with temperature, the precipitation reaction is thermally activating, as termination decreases with temperature. As termination has been largely neglected in previous studies, this phenomenon has yet to be analyzed properly from a mechanistic perspective. These different steady-state responses do not imply, however, any significant differences of the dynamic responses.

Steady–state calculations and stability analysis show that continuous cationic isobutylene polymerization reactors are extremely well behaved. Dynamic instabilities, such as self-sustained oscillatory behavior and steady-state multiplicity, should not be expected in the reactor configurations analyzed, although complex dynamic behavior has been reported for many other polymerization systems, which include free radical solution, free radical emulsion, free radical suspension, and gas-phase and slurry Ziegler–Natta reactors. It seems that the reason why isobutylene reactors are so well behaved is that both the energy balance and the reaction rates are coupled very weakly. Reaction is accomplished almost instantaneously and does not depend very much on the reactor temperature, which may be seen by checking the activation energies in Table II. The plant capacity depends mostly on the heat transfer area available to remove the heat of reaction and not on the reaction rates. So, one important positive feedback mechanism—the thermal positive feedback—is turned off in the cationic isobutylene polymerization. It seems that viscosity effects cannot explain complex dynamic behavior in the reaction systems analyzed either. At heterogeneous reactors, the viscosity of the mixture changes very little due to polymer precipitation, which keeps the viscosity of the reaction mixture close to the viscosity of the solvent. At homogeneous reactors, the viscosity tends to brake the speed of variation of process conditions. As already discussed, when temperature increases viscosity decreases, leading to an increase of the heat transfer coefficient, and vice versa.

A question remains open, though: why do industrial reactors oscillate? Many assumptions may be made, which may even include inadequate tuning of controller parameters. However, two important points must be emphasized. First, heat transfer mechanism is usually much more complex at actual industrial plants and may be the source of unusual dynamics. Second, the reaction systems analyzed are very sensitive to the presence of feed impurities and, as already shown by Pinto and Ray,[5] reactor dynamics may be extremely sensitive to changes of the concentrations of impurities in the feed stream. The analysis of these two points must be the subject of future research.

CONCLUSIONS

Based on a mathematical model designed to describe continuous cationic isobutylene polymerization reactors, steady-state solutions were computed and stability analysis was carried out for certain operation conditions, which resemble the Exxon process. It was shown that these reactors are very stable kinetic systems and that they should not lead to dynamic instabilities, such as self-sustained oscillations and steady-state multiplicity. It seems that complex dynamics observed at actual conditions should be linked to external variables, such as heat exchanger operation and design and the presence of impurities in the feed stream, and not to the reaction mechanism.

We thank Polibutenos do Brasil SA for providing process data and for technical support. We also thank CNPq—Conselho Nacional de Desenvolvimento Científico e Tecnológico—for providing scholarships for both authors.

NOMENCLATURE

A_c	effective heat transfer area
A_f	$AlCl_3$ feed concentration
cp	specific heat of the reactive mixture
cp_f	specific heat of the feed stream
C_{pol}	polymer weight concentration
DP	number average degree of polymerization
D_r	reactor diameter
D_T	turbine impeller diameter
h_i	inside film heat transfer coefficient
h_o	outside film heat transfer coefficient
k	thermal conductivity of the reacting mixture
k^c	thermal conductivity of the continuous phase
k^d	thermal conductivity of the disperse phase
M	monomer concentration
M^c	monomer concentration in the continuous phase
M^d	monomer concentration in the disperse phase
M_f	monomer feed concentration
M_M	monomer molecular weight
M_S	solvent molecular weight
$\bar{M}_n$	number average molecular weight
$\bar{M}_w$	weight average molecular weight
N_T	rotational speed of the turbine impeller
Pr	Prandlt number
Q	polydispersity index
q	outlet volumetric flow rate
q_f	volumetric feed flow rate
Re	Reynolds number
$\boldsymbol{R}_M$	monomer reaction rate

R_S	solvent reaction rate
S	solvent concentration
S^c	solvent concentration in the continuous phase
S^d	solvent concentration in the disperse phase
S_f	solvent feed concentration
T	reactor temperature
T_c	coolant temperature
T_f	feed temperature
U	global heat transfer coefficient
V	reactor volume
x_M^c	monomer molar fraction in the continuous phase
x_S^c	solvent molar fraction in the continuous phase

Greek Symbols

α	propagation probability
$(-\Delta H_P)$	heat of polymerization
χ	monomer conversion
χ_M	isobutylene–polyisobutylene Flory–Huggins interaction parameter
χ_S	methyl chloride–polyisobutylene Flory–Huggins interaction parameter
ϕ	volume fraction of the disperse phase
η	viscosity of the reacting mixture
η_0	viscosity of the isobutylene–n-pentane mixture
η^c	viscosity of the continuous phase
η_{sp}	Huggins specific viscosity.
η_w	fluid viscosity at the wall temperature,
$[\eta]$	Mark–Houwink intrinsic viscosity
λ_k	kth moment of dead polymer molecular weight distribution
ν_j	volume fraction of j
$\nu_{M,f}$	monomer feed volume fraction
ν_M^d	monomer disperse phase volume fraction
ν_P^d	polymer disperse phase volume fraction
ν_S^d	solvent disperse phase volume fraction
θ	reactor discharging time
θ_f	reactor charging time
ρ	density of the reactive mixture
ρ_f	density of the feed stream
ρ_M	monomer density
ρ_S	solvent density
$\rho_{M,f}$	monomer density at feed temperature
$\rho_{S,f}$	solvent density at feed temperature
ω_j	mass fraction of species j.
ξ	catalyst efficiency
ξA_f	initiator feed concentration

APPENDIX: JACOBIAN MATRIX

In this appendix the Lyapunov First Method for ordinary differential equations and an extension for differential algebraic systems are presented. Assuming that the Implicit Function Theorem conditions are satisfied,[40] the DAE jacobian matrix may be written as:[43]

$$\underline{\underline{J}} = \left(\frac{\partial \dot{\underline{x}}}{\partial \underline{x}}\right)^{\cdot} \tag{A.1}$$

where the external dot means that algebraic restrictions of the differential algebraic system are satisfied.

INTRODUCTION

The classical Lyapunov Theory[44] allows the analysis of the stability of dynamic system responses. Let an autonomous system be described by the following set of ordinary differential equations:

$$\frac{d\underline{x}}{dt} = \dot{\underline{x}} = \underline{g}(\underline{x}) \tag{A.2}$$

Let $\underline{x}^*$ be a steady-state solution of (A.2):

$$\underline{g}(\underline{x}^*) = \underline{g}^* = 0 \tag{A.3}$$

If the steady state is perturbed, then

$$\underline{x} = \underline{x}^* + \delta\underline{x} \tag{A.4}$$

$$\delta\dot{\underline{x}} = \underline{g}^* + D_{\underline{x}}^* \underline{g} \cdot \delta\underline{x} + \underline{h}(\delta\underline{x}) \tag{A.5}$$

where $D_{\underline{x}}^* \underline{g}$ is the jacobian matrix of (A.2), evaluated at the steady state $\underline{x}^*$, and $\underline{h}(\delta\underline{x})$ are the nonlinear higher order terms of (A.2).

Assuming that the perturbation is small:

$$\delta\dot{\underline{x}} \cong D_{\underline{x}}^* \underline{g} \cdot \delta\underline{x} \tag{A.6}$$

The stability of the steady-state solutions (A.2) is completely determined by the signs of the $D_{\underline{x}}^* \underline{g}$ eingenvalues. Thus, $\underline{x}^*$ is: a stable steady state, if the real parts of all $D_{\underline{x}}^* \underline{g}$ eingenvalues are strictly negative; an unstable steady state, if at least one of the $D_{\underline{x}}^* \underline{g}$ eingenvalues has a strictly positive real part.

If the real part of one or more of the $D_{\underline{x}}^* \underline{g}$ eingenvalues is equal to zero, the system stability is determined by the higher order terms. At these points, a radical change of system dynamics occurs.

These points are the focus of the Local Bifurcation Theory.[40]

SOLUTION POLYMERIZATION REACTOR MODEL

The solution polymerization reactor model is described by a system of autonomous differential algebraic equations in the form:

$$\dot{\underline{x}} = \underline{g}(\underline{x}, \theta) \tag{A.7a}$$

$$0 = h(\dot{\underline{x}}, \underline{x}, \theta) \tag{A.7b}$$

where:

$$\underline{x}^{\mathrm{T}} \equiv [\mathrm{M}, \mathrm{S}, \mathrm{T}, \lambda_1, \lambda_2] \tag{A.8a}$$

and

$$\theta \equiv \theta_e \tag{A.8b}$$

Expanding (A.7) into a Taylor series and neglecting higher order terms:

$$\delta\dot{\underline{x}} = D^*_{\underline{x}}\underline{g} \cdot \delta\underline{x} + D^*_{\theta}\underline{g} \cdot \delta\theta \tag{A.9a}$$

$$0 = D^*_{\underline{x}}h \cdot \delta\underline{x} + D^*_{\dot{\underline{x}}}h \cdot \delta\dot{\underline{x}} + D^*_{\theta}h \cdot \delta\theta \tag{A.9b}$$

From eq. (A.9b) one can write $\delta\theta$ as a function of $\delta\underline{x}$ and $\delta\dot{\underline{x}}$:

$$\delta\theta = -[D^*_{\theta}h]^{-1} \cdot [D^*_{\underline{x}}h \cdot \delta\underline{x} + D^*_{\dot{\underline{x}}}h \cdot \delta\dot{\underline{x}}] \tag{A.10}$$

which may be substituted in (A.9a):

$$\delta\dot{\underline{x}} = D^*_{\underline{x}}\underline{g} \cdot \delta\underline{x} + D^*_{\theta}\underline{g} \times [-[D^*_{\theta}h]^{-1} \cdot [D^*_{\underline{x}}h \cdot \delta\underline{x} + D^*_{\dot{\underline{x}}}h \cdot \delta\dot{\underline{x}}]] \tag{A.11}$$

or

$$\delta\dot{\underline{x}} = [\underline{\underline{I}} + \mathrm{D}^*_{\theta}\underline{g} \cdot [D^*_{\theta}h]^{-1} \cdot D^*_{\dot{\underline{x}}}h]^{-1} \times [D^*_{\underline{x}}\underline{g} - D^*_{\theta}\underline{g} \cdot [D^*_{\theta}h]^{-1} \cdot D^*_{\underline{x}}h] \cdot \delta\underline{x} \tag{A.12}$$

Thus, the Jacobian of the solution polymerization reactor model is

$$\underline{\underline{J}} = [\underline{\underline{I}} + D^*_{\theta}\underline{g} \cdot [D^*_{\theta}h]^{-1} \cdot D^*_{\dot{\underline{x}}}h]^{-1} \times [D^*_{\underline{x}}\underline{g} - D^*_{\theta}\underline{g} \cdot [D^*_{\theta}h]^{-1} \cdot D^*_{\underline{x}}h] \tag{A.13}$$

PRECIPITATION POLYMERIZATION REACTOR MODEL

The precipitation reactor model is described by a set of autonomous differential algebraic equations in the form:

$$\frac{d\underline{f}(\underline{x}, y)}{dt} = \underline{g}(\underline{x}, y, \theta) \tag{A.14a}$$

$$0 = h(\underline{x}, y) \tag{A.14b}$$

where (A.14a) represents the four reactor balance equations and (A.14b) represents the thermodynamic equilibrium equation. The state variables are:

$$\underline{x}^{\mathrm{T}} \equiv [\nu^c_{\mathrm{M}}, \phi, \mathrm{T}] \tag{A.15a}$$

$$y \equiv \nu^d_{\mathrm{P}} \tag{A.15b}$$

$$\theta = \theta_e \tag{A.15c}$$

In this case, it is convenient to define a set of variables $\underline{z}$, which represents the functions inside the time derivatives:

$$\dot{\underline{z}} = \underline{g}(\underline{x}, y, \theta) \tag{A.16a}$$

$$\underline{z} = \underline{f}(\underline{x}, y) \tag{A.16b}$$

$$0 = h(\underline{x}, y) \tag{A.16c}$$

Expanding (A.16) into a Taylor series and neglecting higher order terms:

$$\delta\dot{\underline{z}} = D^*_{\underline{x}}\underline{g} \cdot \delta\underline{x} + D^*_{y}\underline{g} \cdot \delta y + D^*_{\theta}\underline{g} \cdot \delta\theta \tag{A.17a}$$

$$\delta\underline{z} = D^*_{\underline{x}}\underline{f} \cdot \delta\underline{x} + D^*_{y}\underline{f} \cdot \delta y \tag{A.17b}$$

$$0 = D^*_{\underline{x}}h \cdot \delta\underline{x} + D^*_{y}h \cdot \delta y \tag{A.17c}$$

Substituting (A.17b) in (A.17a):

$$D^*_{\underline{x}}\underline{f} \cdot \delta\dot{\underline{x}} + D^*_{y}\underline{f} \cdot \delta\dot{y} = D^*_{\underline{x}}\underline{g} \cdot \delta\underline{x} + D^*_{y}\underline{g} \cdot \delta y + D^*_{\theta}\underline{g} \cdot \delta\theta \tag{A.18}$$

From (A.17c) one can write δy as a function of $\delta\underline{x}$:

$$\delta y = [D^*_{y}h]^{-1} \cdot D^*_{\underline{x}}h \cdot \delta\underline{x} \tag{A.19}$$

which may be substituted in (A.18), leading to:

$$[D^*_{\underline{x}}\underline{f} - D^*_{y}\underline{f} \cdot [D^*_{y}h]^{-1} \cdot D^*_{\underline{x}}h] \cdot \delta\dot{\underline{x}} = [D^*_{\underline{x}}\underline{g} + D^*_{y}\underline{g} \cdot [D^*_{y}h]^{-1} \cdot D^*_{\underline{x}}h]\delta\underline{x} + D^*_{\theta}\underline{g} \cdot \delta\theta \tag{A.20}$$

In this system the matrices that multiply $\delta\underline{x}$ and $\delta\underline{\dot{x}}$ are 4×3 noninvertible matrices. Therefore, it is possible to write $\delta\theta$ as an explicit function of $\delta\underline{x}$ and $\delta\underline{\dot{x}}$, using one of the four (linear) equations that constitute (A.20). Then, let:

$$\underline{\underline{A}} = [D^*_{\underline{x}}\underline{f} - D^*_{\underline{y}}\underline{f}\cdot[D^*_{\underline{y}}h]^{-1} \times D^*_{\underline{x}}h] = \begin{bmatrix} \underline{\underline{D}} \\ \dots \\ \underline{d}^{\mathrm{T}} \end{bmatrix} \quad \text{(A.21a)}$$

$$\underline{\underline{B}} = [D^*_{\underline{x}}\underline{g} + D^*_{\underline{y}}\underline{g}\cdot[D^*_{\underline{y}}h]^{-1} \times D^*_{\underline{x}}h] = \begin{bmatrix} \underline{\underline{E}} \\ \dots \\ \underline{e}^{\mathrm{T}} \end{bmatrix} \quad \text{(A.21b)}$$

$$\underline{C} = D^*_{\theta}\underline{g} = \begin{bmatrix} \underline{F} \\ \dots \\ f \end{bmatrix} \quad \text{(A.21c)}$$

where $\underline{\underline{A}}$ and $\underline{\underline{B}}$ are 4×3 matrices, $\underline{\underline{D}}$ and $\underline{\underline{E}}$ are square 3×3 matrices, $\underline{C}$ is a four-dimensional column vector, $\underline{d}$, $\underline{e}$, and $\underline{F}$ are three-dimensional column vectors, and f is a escalar.

Then:

$$\underline{\underline{A}}\cdot\delta\underline{\dot{x}} = \underline{\underline{B}}\cdot\delta\underline{x} + \underline{C}\cdot\delta\theta \quad \text{(A.22)}$$

or:

$$\underline{\underline{D}}\cdot\delta\underline{\dot{x}} = \underline{\underline{E}}\cdot\delta\underline{x} + \underline{F}\cdot\delta\theta \quad \text{(A.23a)}$$

$$\underline{d}^{\mathrm{T}}\cdot\delta\underline{\dot{x}} = \underline{e}^{\mathrm{T}}\cdot\delta\underline{x} + f\cdot\delta\theta \quad \text{(A.23b)}$$

From (A.23b), and assuming f is not null:

$$\delta\theta = \frac{\underline{d}^{\mathrm{T}}}{f}\cdot\delta\underline{\dot{x}} - \frac{\underline{e}^{\mathrm{T}}}{f}\cdot\delta\underline{x} \quad \text{(A.24)}$$

which may be substituted in (A.23a), leading to:

$$\underline{\underline{D}}\cdot\delta\underline{\dot{x}} = \underline{\underline{E}}\cdot\delta\underline{x} + \underline{F}\cdot\left[\frac{\underline{d}^{\mathrm{T}}}{f}\cdot\delta\underline{\dot{x}} - \frac{\underline{e}^{\mathrm{T}}}{f}\cdot\delta\underline{x}\right] \quad \text{(A.25)}$$

or

$$\left[\underline{\underline{D}} - \frac{\underline{F}\cdot\underline{d}^{\mathrm{T}}}{f}\right]\cdot\delta\underline{\dot{x}} = \left[\underline{\underline{E}} - \frac{\underline{F}\cdot\underline{e}^{\mathrm{T}}}{f}\right]\cdot\delta\underline{x} \quad \text{(A.26)}$$

Assuming that

$$\left[\underline{\underline{D}} - \frac{\underline{F}\cdot\underline{d}^{\mathrm{T}}}{f}\right]$$

is invertible:

$$\delta\underline{\dot{x}} = \left[\underline{\underline{D}} - \frac{\underline{F}\cdot\underline{d}^{\mathrm{T}}}{f}\right]^{-1}\cdot\left[\underline{\underline{E}} - \frac{\underline{F}\cdot\underline{e}^{\mathrm{T}}}{f}\right]\cdot\delta\underline{x} \quad \text{(A.27)}$$

Thus, the Jacobian of the precipitation polymerization reactor model is

$$\underline{J} = \left[\underline{\underline{D}} - \frac{\underline{F}\cdot\underline{d}^{\mathrm{T}}}{f}\right]^{-1}\cdot\left[\underline{\underline{E}} - \frac{\underline{F}\cdot\underline{e}^{\mathrm{T}}}{f}\right] \quad \text{(A.28)}$$

where $\underline{d}$, $\underline{e}$, f, $\underline{\underline{D}}$, $\underline{\underline{E}}$, and $\underline{F}$ are defined by eq. (A.21).

REFERENCES

1. E. N. Kresge, R. Schatz, and H. C. Wang, *Encyclopedia of Polymer Science and Technology.* 2nd ed. Wiley, New York, 1987, p. 423.
2. J. P. Kennedy and E. Maréchal, *Carbocationic Polymerization,* Wiley, New York, 1982.
3. C. Dinucci, Personal Communications to J. C. Pinto, 1992–1994.
4. J. C. Pinto and W. H. Ray, *Chem. Eng. Sci.,* **50,** 715 (1995).
5. J. C. Pinto and W. H. Ray, *Chem. Eng. Sci.,* **50,** 1041 (1995).
6. J. C. Pinto and W. H. Ray, *Chem. Eng. Sci.,* **51,** 63 (1996).
7. L. S. Henderson and R. A. Cornejo, *Ind. Eng. Chem. Res.,* **28,** 1644 (1989).
8. K. J. Kim, K. Y. Choi, and J. C. Alexander, *Polym. Eng. Sci.,* **32,** 494 (1992).
9. A. D. Schmidt and W. H. Ray, *Chem. Eng. Sci.,* **36,** 1401 (1981).
10. J. C. Pinto, *Polym. Eng. Sci.,* **30,** 291 (1990).
11. K. Y. Choi and W. H. Ray, *Chem. Eng. Sci.,* **40,** 2261 (1985).
12. L. Marini and C. Georgakis, *AIChE J.,* **30,** 401 (1984).
13. G. Maschio, F. Artigiani, M. Di Mania, and P. Giusti, *J. Appl. Polym. Sci.,* **29,** 1215 (1984).
14. J. P. Kennedy and R. M. Thomas, *J. Polym. Sci.,* **45,** 227 (1960).
15. J. P. Kennedy and R. M. Thomas, *J. Polym. Sci.,* **46,** 233 (1960).
16. J. P. Kennedy and R. M. Thomas, *J. Polym. Sci.,* **46,** 481 (1960).
17. J. P. Kennedy and R. M. Thomas, *J. Polym. Sci.,* **49,** 189 (1961).
18. J. P. Kennedy and R. M. Thomas, *J. Polym. Sci.,* **55,** 311 (1961).
19. J. P. Kennedy, I. Kirshenbaum, R. M. Thomas, and D. C. Murray, *J. Polym. Sci., Part A: Chem. Ed.,* **1,** 331 (1963).
20. J. P. Kennedy and R. G. Squires, *Polymer,* **6,** 579 (1965).

21. J. P. Kennedy and R. G. Squires, *J. Macromol. Sci. Chem.*, **A1,** 805 (1967).
22. J. P. Kennedy, *Polymer Chemistry of Synthetic Elastomers,* J. P. Kennedy, and E. G. N. Törnqvist, Eds., Wiley, New York, 1968, p. 291.
23. I. Kirshenbaum, J. P. Kennedy, and R. M. Thomas, *J. Polym. Sci. Part A: Chem. Ed.*, **1,** 789 (1963).
24. M. F. Freitas, M.Sc. Thesis, COPPE/UFRJ, 1994.
25. P. H. Plesch, *Makromol. Chem.*, **175,** 1065 (1974).
26. C. E. Schildknecht, *Polymer Processes,* C. E. Schildknecht, Ed., Interscience, New York, 1960, p. 199.
27. D. R. Athey, *Proc. UK Conf. Heat Transf.*, **2,** 1297 (1988).
28. Luyben *AIChE J.* **12,** 662 (1966)
29. J. Brandrup and E. H. Immergut, *Polymer Handbook,* 3rd ed., Wiley, New York, 1989.
30. D. Q. Kern, *Process Heat Transfer,* McGraw-Hill, New York, 1960.
31. H. F. Rase, *Chemical Reactor Design for Process Plants,* Wiley, New York, 1977.
32. E. S. Chapman, H. Dallenbach, and F. A. Holland, *Trans. Instn. Chem. Eng.*, **42,** T398 (1964).
33. D. W. Van Krevelen and P. J. Hoftyzer, *Properties of Polymers: Correlations with Chemical Structure,* Elsevier, Amsterdan, 1972.
34. R. C. Reid, J. M. Prausnitz, and B. E. Poling, *The Properties of Gases and Liquids,* 3rd ed., MacGraw-Hill, New York, 1987.
35. K. Eiermann and K. H. Hellwege, *J. Polym. Sci.*, **57,** 99 (1962).
36. Y. S. Touloukian, P. E. Liley, and S. C. Saxena, *Conductivity: Nonmetallic Liquids and Gases,* Plenum Publishing, New York, 1970.
37. Y. S. Touloukian and T. Makita, *Specific Heat: Nonmetallic Liquids and Gases,* Plenum Publishing, New York, 1970.
38. A. F. M. Barton, *CRC Handbook of Solubility Parameters and Other Cohesion Parameters,* CRC Press, Boca Raton, 1983.
39. F. Frantisek, J. W. Smith, and J. Dohnal, *Ind. Eng. Chem. Processes Des. Dev.*, **7,** 188 (1968).
40. R. Seydel, *From Equilibrium to Chaos: Practical Bifurcation and Stability Analysis,* Elsevier, New York, 1988.
41. M. Kubicek, *ACM TOMS,* **2,** 98 (1976).
42. H. P. Press, B. P. Flannery, S. A. Teukolsky, and W. T. Vetterling, *Numerical Recipes in C: The Art of Scientific Computing,* Cambridge University Press, Cambridge, 1988.
43. W. D. Seider, D. D. Brengel, and S. Widagdo, *AIChE J.*, **37,** 1 (1991).
44. P. Hagedron, *Oscilações Não Lineares,* Edgard Blücher, São Paulo, 1984.

Received June 14, 1995
Accepted October 5, 1995